Thermodynamic Interaction Parameter of Star–Star Polybutadiene Blends

T. D. MARTTER, M. D. FOSTER, T. YOO, S. XU, G. LIZARRAGA, R. P. QUIRK

The University of Akron, Maurice Morton Institute of Polymer Science, Akron, Ohio 44325

Received 31 May 2002; revised 10 October 2002; accepted 22 October 2002

ABSTRACT: The value of the thermodynamic interaction parameter, χ_{eff}, for star–star polybutadiene blends was determined with small-angle neutron scattering. Blends in which the stars have the same number of arms and blends in which the stars have different numbers of arms are investigated. For star–star isotopic blends with components having the same number of arms, the presence of the junction point of the star leads to a value of χ_{eff} that is larger than that for an analogous linear–linear isotopic blend. However, changes in the value of χ_{eff} resulting from small dissimilarities in the number of arms of the two components in the isotopic star–star blends were too small to resolve. © 2002 Wiley Periodicals, Inc. J Polym Sci Part B: Polym Phys 41: 247–257, 2003
Keywords: star polymers; thermodynamics; blends; polybutadiene; neutron scattering

INTRODUCTION

The creation of polymers with architectures incorporating regular long-chain branching provides opportunities for tailoring polymer physical properties; blends containing long-branched polymer components are already in commercial use. A fundamental issue related to such blends is the degree to which the branching of one component may compromise thermodynamic miscibility in the system, even when the blend components are made from the same monomer, that is, when the components differ only in architecture. The degree of miscibility can be characterized with an effective thermodynamic exchange interaction parameter, χ_{eff}. A Gaussian field theory by Fredrickson et al.[1] has predicted that the architectural differences between linear and long-branched components do not readily lead to bulk-phase immiscibility but do result in a measurable increase in the value of χ_{eff} over that of a comparable linear–linear polymer blend.

Such thermodynamic effects may be investigated either by mapping phase diagrams or by measuring the value of χ_{eff} under conditions of interest. The first approach has the disadvantage that one must first explore the parameter space of blend component molecular characteristics to find pairs that phase-separate in an experimentally available window of temperature. Small-angle neutron scattering (SANS) should be an effective tool for pursuing the second approach, as SANS has been used extensively to measure the value of χ_{eff} in binary blends of linear chains. The scattering-structure factor for a binary blend of linear polymers is given by DeGennes[2] in the random phase approximation (RPA) as

$$S^{-1}(q) = \frac{1}{\phi_a N_a P(R_{g,a},q)} + \frac{1}{\phi_b N_b P(R_{g,2},q)} - 2\chi_{eff} \quad (1)$$

where ϕ_i is the volume fraction of species i, N_i is the number of segments in the polymer i, and χ_{eff} is the effective thermodynamic interaction pa-

Correspondence to: M. D. Foster (E-mail: mfoster@uakron.edu)

Journal of Polymer Science: Part B: Polymer Physics, Vol. 41, 247–257 (2003)

rameter, which we take here as a good estimate of the bare interaction parameter. $P(R_g,q)$ is the Debye form factor that captures the characteristic form of the linear chain in the melt. For blends in which the architecture of a component is nonlinear, the form of the form factor must be appropriately modified.

In the particular case that the two components have the same repeat unit chemistry, the contrast necessary to perform the SANS measurement can be achieved by deuterating one of the components. However, an isotopic linear–linear blend is characterized by a measurable value of χ_{eff} solely because of labeling.[3–6] This labeling effect must be properly accounted for when examining thermodynamic interactions because of architectural effects that are anticipated to be small in magnitude for low degrees of long-chain branching.[1] The magnitude of χ_{eff} may also be influenced by differences in microstructure[7–9] and chain-end functionalization.[10]

Phase behavior and scattering studies[11–20] on the effect of architecture on the bulk thermodynamics of blends of branched and linear polymer chains offer a consensus that architecture effects are measurable and can be large enough for bulk-phase separation in some circumstances. Blends of linear chains with the following three types of branched chains have been considered: random short-chain branched chains,[11] comb-branched chains,[12] and regular star-branched chains.[13–20]

Greenberg and coworkers[17–19] used SANS to measure values of χ_{eff} for blends of star and linear polystyrene (PS) and attempted to quantify changes in the interaction because of architecture with changes in the number of arms. From values of χ_{eff}, they derived estimates of the interaction because of architectural effects alone, χ_ϵ, by measuring separately the interaction because of isotopic labeling alone. χ_ϵ increased with the number of arms of the star. Changes with the number of arms showed the qualitative behavior expected from Gaussian field theory,[1] but there was near quantitative agreement only for the case for a four-arm star; overall the experimental values of χ_ϵ were substantially lower than those calculated from theory.[21] Martter et al.[20] measured the value of χ_{eff} for blends of star and linear polybutadiene (PB) polymers with SANS and found that χ_{eff} and χ_ϵ varied nonmonotonically with an increase in the number of arms from 4 to 12. This result contrasted with the expectation from the theory of Fredrickson et al.[1] that an increase in χ_ϵ with the number of arms of the star should be universally observed regardless of the chemical structure of the repeat unit.

This contribution probes the thermodynamic interactions present in blends containing two regular star-branched components that may have the same number of arms or different numbers of arms. Two previous SANS studies of star–star homopolymer blends[22,23] may be found in the literature. Both focus on SANS for the characterization of the conformation of a single star in a melt of stars to address the question of how that conformation might vary from that anticipated by a Gaussian approximation. Horton et al.[22] investigated the value of R_g for the entire star-branched polyethylenes (PEs) with 3–18 arms and various arm molecular weights. They measured blends of ~50 wt % partially deuterated PE stars with very closely matched hydrogenous PE stars with equal numbers of arms. To derive values of the radius of gyration of the stars, they ignored the presence of thermodynamic interactions because of labeling and assumed that the form factors for the hydrogenous and deuterated stars were identical. In this case the experimental intensity should be given by the single pertinent form factor multiplied by a constant. Further assuming that the arms of the stars were not stretched, they fit the data with the Benoît form factor[24] for stars with Gaussian arms, allowing the overall R_g of the stars to vary as a fitting parameter. In this way, they discovered that experimental estimates for R_g exceeded what would be expected for stars with arms having Gaussian conformations. The value of R_g for the entire molecule increased by 30% over the expectation from a Gaussian model value for the case of a 12-arm star with a weight-average molecular weight (M_w) of 9 k. However, for a 12-arm star with a molecular weight of 186 k, the increase in R_g was slightly less than 10%. The effect of swelling depended on the molecular weight of the arms for the 12-arm stars.

Hutchings et al.[23] investigated 3-, 4-, 8-, and 12-arm star PB melts containing a single star component. One arm of the star was deuterated to enable the determination of the R_g of that arm. They reported that the arms in 3-, 4-, 8-, and 12-arm stars of a melt were all stretched, with the degree of stretching increasing with the number of arms. The R_g of the deuterated arm of the 8-arm star with arm molecular weight of 33 k was 8% larger than the value expected from the Gaussian approximation, and for the 12-arm star with 31 k arms the stretching increased to 30%. Apprehending the significance of the results is

complicated by the fact that the authors introduced two interaction parameters into the SANS data analysis to extract values of R_g for the individual arms with this labeling scheme. The interaction between the deuterated arm and the other arms of the star, χ_{HD}, decreased initially when the number of arms was increased from three to eight. When the number of arms reached 12, χ_{HD} increased. The opposite behavior was found for χ_{DM}, the interaction between the deuterated arm and the matrix. No explicit analysis of the degree of coupling between the parameters in the data analysis was offered.

Two issues of the thermodynamics of star–star blends are addressed in this work. First, the value of χ_{eff} in a star–star blend just because of isotopic labeling was measured to determine if χ_{eff} is the same as that seen for isotopic linear–linear blends. This question was addressed by determining a single interaction parameter with SANS for blends of hydrogenous stars mixed with deuterated stars with the same number of arms. Second, the value of χ_{eff} was measured for star–star blends in which the components had different numbers of arms to determine how this structural asymmetry affected the value of χ_{eff}.

EXPERIMENTAL

Synthesis

The hydrogenous star polybutadiene (hPB) and deuterated star polybutadiene (dPB) polymers with 4, 6, 8, and 12 arms were synthesized by living anionic polymerization at The University of Akron. The poly(butadienyllithium) arm precursors of well-defined molecular weight were synthesized in cyclohexane with *sec*-butyllithium initiator and then linked together with the appropriate linking agent to form stars.[25] The linking agents used to form the 4-, 6-, 8-, and 12-arm stars were silicon tetrachloride, 1,2-bis(trichlorosilyl)hexane, tetrakis[2-(dichloromethylsilyl)ethyl]-silane, and tetra(trichlorosilylethane)silane, respectively. Linking of the arms was performed with an excess of arm to drive the reaction to completion. This excess was later removed by multiple fractionations from 0.5 wt % polymer solutions in toluene with methanol as the nonsolvent. The number of arms in the star was determined by first characterizing the arm precursor and then the complete star by gel permeation chromatography with the following three inline detectors: a viscometer, a refractometer, and light scattering. Molecular weights were confirmed with light scattering in a separate laboratory. Intrinsic viscosity measurements were performed for all star polymers in toluene at 35 °C, and values of the branching factor,[26] g', were calculated. The *branching factor* is defined as the ratio of intrinsic viscosities of the branched and linear species of equal overall molecular weight, $g' = [\eta]_b/[\eta]_l$. The experimental values of g' (reported previously[20]) compared well with published experimental results,[26,27] indicating that the numbers of arms of the stars are very close to the intended values. Oxidation of the samples was slowed dramatically by the addition of <1 wt % of the antioxidant 2,6-di-*tert*-butyl-4-methylphenol and by keeping the samples in the dark in a freezer or over dry ice whenever they were not being measured. The degree of 1,4-addition in the polymers was kept nearly constant and was generally close to 94% as determined by ^{1}H NMR for the hydrogenous stars. The microstructure for the deuterated stars was checked with ^{1}H NMR (with the presence of residual ^{1}H atoms located randomly in the chains) and varied slightly among the stars, but was consistently slightly smaller than that of the hydrogenous stars although the same conditions were used for the synthesis of hydrogenous and deuterated stars. The greatest deviations from the target microstructure are seen for the 4-arm and 12-arm deuterated stars. The implications of the small microstructure mismatch in blends containing one of those two components are dealt with in the results and discussion. The molecular characteristics of all the PBs are listed in Table 1.

SANS Sample Preparation

Binary blends of about 18 and 82 wt % star PB were dissolved in filtered toluene (filtered twice with a 0.02 μm filter) in a Teflon® beaker. This blend composition was chosen for ready comparison with results from star–linear blends.[20] Because one component of the blend must be labeled with deuterium, an "isotopic swap" analogue of each sample was also prepared. The majority of the solvent was removed by evaporation at ambient conditions for 1 day. The samples were then further dried under roughing vacuum at room temperature for at least 3 days. Each dried sample was pressed into a brass-ring spacer of i.d. 10 mm and thickness of 1.0 mm and then placed between quartz windows into a standard reusable

Table 1. Molecular Characteristics of Polybutadiene Polymers

Polymer	Name	M_n (g/mol)[a]	N[b]	M_n/M_n	1,4-Addition[c] (%)
Polybutadiene	hPB	86,500	1620	1.04	94
Deuterated PB	dPB	98,000	1640	1.06	~82
4-Arm star	h4s	95,000	1780	1.03	94
6-Arm star	h6s	121,000	2270	1.01	94
8-Arm star	h8s	114,000	2140	1.06	93
12-Arm star	h12s	107,000	2000	1.01	94
4-Arm deuterated star	d4s	97,000	1620	1.04	86
6-Arm deuterated star	d6s	110,000	1860	1.02	92
8-Arm deuterated star	d8s	113,000	1890	1.01	93
12-Arm deuterated star	d12s	116,000	1950	1.02	86

[a] Determined by GPC with three inline detectors: viscometer, refractometer, and light scattering.
[b] Number of segments determined with a segment volume of 60 cm^3/mol.
[c] Determined by ^1H NMR.

brass sample holder. A list of the blends studied is given in Table 2.

Instrumentation

SANS measurements were performed on the NG3 30 m SANS instrument at the Cold Neutron Research Facility at the National Institute of Standards and Technology (NIST) (Gaithersburg, MD). The nominal wavelength of the neutron beam was 6 Å with a resolution ($\Delta\lambda\lambda$) of 0.150 full width at half-maximum. A sample-to-detector distance of 13 m and a detector offset of 20 cm were used with a 2-in. diameter beamstop, one neutron guide, and a sample aperture of 0.635 cm to yield an accessible range of the scattering vector, $\mathbf{q}$ ($= 4\pi\sin\theta/\lambda$), of 0.005–0.05 $Å^{-1}$. The samples were placed inside a temperature-controlled, remotely controlled, seven-position aluminum sample changer that was located in an aluminum vacuum chamber. The chamber was evacuated (to 450 μm Hg) and then backfilled with nitrogen gas to obtain a slight positive pressure, and this positive pressure was maintained throughout the measurement. The temperature was varied in steps of 30 °C monotonically between 40 and 160 °C, with the temperature maintained at ±0.1 °C of each setpoint value. A thermal equilibration time of 15 min was allowed at each temperature before collecting data. The integral intensity of the scattered beam was equilibrated in about 5 min.

Table 2. Molecular Characteristics of SANS Samples

	Polymer 1		Polymer 2	$\chi_{eff} = A/T + B$	
Blend	Name	ϕ	Name	A	$B \times 10^4$
h4d4s	4-Arm hpb	0.19	4-Arm dpb	.41	−5.40
d4h4s	4-Arm dpb	0.17	4-Arm hpb	.33	−2.74
h6d6s	6-Arm hpb	0.20	6-Arm dpb	.34	−4.39
d6h6s	6-Arm dpb	0.18	6-Arm hpb	.27	−1.79
h8d8s	8-Arm hpb	0.19	8-Arm dpb	.34	−3.22
d8h8ss	8-Arm dpb	0.16	8-Arm hpb	.30	−2.74
d12h12s	12-Arm dpb	0.16	12-Arm hpb	.30	−0.72
h4d6s	4-Arm hpb	0.20	6-Arm dpb	.46	−6.65
d4h6s	4-Arm dpb	0.16	6-Arm hpb	.37	−4.02
h4d8s	4-Arm hpb	0.20	8-Arm dpb	.46	−6.66
d4h8s	4-Arm dpb	0.17	8-Arm hpb	.34	−3.26
h6d8s	6-Arm hpb	0.20	8-Arm dpb	.32	−3.52
d6h8s	6-Arm dpb	0.16	8-Arm hpb	.29	−1.66

Data were collected with the beam blocked and with the instrument empty for estimating the background contributions. Because the samples were mounted in cells with quartz windows, the scattering from an empty cell was also measured. To correct for incoherent scattering, a 100% hPB sample was measured. Transmission coefficients were measured for all samples at each temperature, both to optimize the normalization to absolute scattering at each temperature and as a simple check for the development of bubbles. To convert the data into absolute intensities, an isotopic polymer blend standard sample was also measured. The raw data were azimuthally averaged and then converted to absolute coherent scattering intensity as a function of **q**.

SANS Data Analysis

The scattering data for all SANS samples were fit with the RPA approach with structure factors for the star polymers that assume Gaussian behavior of the arms. The measured absolute coherent scattering intensity, $I(\mathbf{q})$, is related to the structure factor, $S(\mathbf{q})$, by

$$I(\boldsymbol{q}) = \frac{(b_a - b_b)^2}{V} S(\boldsymbol{q}) \tag{2}$$

where b_i is the coherent scattering length of polymer i, V is the polymer segment volume, **q** is the scattering vector, and $S(\mathbf{q})$ is the overall structure factor for the blend given in eq 1. A segment volume of 60 cm^3/mol was used at 40 °C. The coherent scattering lengths for hPB and dPB were calculated as 4.13×10^{-13} and 6.66×10^{-12} cm. Benoît derived a form factor for the case of a star-branched polymer[24] in which the arms remain Gaussian to give

$$P(\boldsymbol{q}) = \frac{2}{p u_r^4}\left[u_r^2 - (1 - e^{-u_r^2}) + \frac{p-1}{2}(1 - e^{-u_r^2})^2\right] \tag{3}$$

where

$$u_r^2 = \frac{Na^2q^2}{6} = \boldsymbol{q}^2\langle R_g^2\rangle_a \tag{4}$$

and p is the number of arms, N is the number of segments in an arm of the star, and the subscript "a" denotes a quantity defined for one arm. The segment length for linear PB[4] with comparable microstructure has been measured as 6.9 Å, and did not vary appreciably with temperature.[28] A value of 6.69×10^{-4} K^{-1} for the thermal-expansion coefficient[29] was used to adjust the molar volume with changing temperature.

If the Gaussian approximation is maintained, the only parameter that is unknown in these equations is χ_{eff}, and its value can then be determined by modeling the scattering curves with χ_{eff} as an adjustable parameter. Because previous work has suggested that the star dimensions could be somewhat larger than the Gaussian dimensions for larger numbers of arms, one could attempt to allow the values of R_g to vary as a first-order attempt at capturing the effects of stretching. We chose not to do this because for all the samples used here, the R_g of each component would have to be allowed to vary, leading to a total number of adjustable parameters of three. In our estimation the uncertainty introduced by increasing the number of adjustable parameters outweighs the potential advantage of more accurately accounting for the structure factor of the star chain. Stretching should not be a serious issue for stars with only four or six arms. As a check, R_g for the deuterated 12-arm star was determined independently with a Guinier analysis of data from a dilute (1%) sample of d-star in h-star matrix. This yielded a value of 61 ± 2 Å for this star for which a calculation assuming a Gaussian conformation predicts R_g = 60 ± 2 Å (uncertainty because of molecular weight measurement). Thus, we have not attempted to explicitly account for stretching, although in the general case one anticipates some degree of stretching may be present. Sample scattering curves for a blend of 19 vol % four-arm star hPB and 81 vol % four-arm star dPB (h4d4s) are shown with model fits for temperatures of 40, 100, and 160 °C in Figure 1. From this point forward, all concentrations will be presented as volume fractions or percentages. To achieve the agreement seen here between the model and the experimental data, a prefactor of order unity was used to adjust the model. Slight deviations between the model and the experimental data are seen at the lowest values of **q** considered.

RESULTS AND DISCUSSION

Stars with the Same Numbers of Arms

Scattering was measured for the following three h-star/d-star PB blends of similar composition in

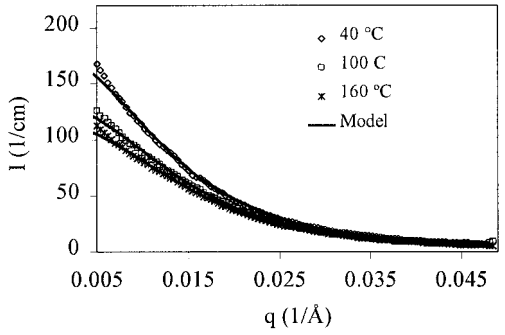

Figure 1. SANS experimental data with fits to RPA for a blend of 19 vol % four-arm star hPB in a matrix of 81 vol % linear dPB (h4d4s) at 40, 100, and 160 °C.

which the number of arms in the two components was the same: (1) four-arm star hPB/four-arm star dPB (h4d4s), (2) six-arm star hPB/six-arm star dPB blend (h6d6s), and (3) eight-arm star hPB/eight-arm star dPB blend (h8d8s). The prefactor used for h8d8s to achieve good agreement between the experimental data and model was much smaller than the values used for the other two samples, which were close to unity. This suggests some difficulty with that sample, and therefore the values of χ_{eff} for h8d8s are the least reliable. Temperature dependencies of χ_{eff} for these samples are portrayed in Figure 2, along with those for a 20/80 linear hPB (87 k)/linear dPB (98 k) blend (18hll). Because all the data given here for star–star blends were measured at the same beam time and under identical conditions, systematic errors due to calibration of intensity should be the same for all star–star data. Therefore, random errors due to error in molecular weight determination and number of arms in the star are the sources of uncertainty of greatest interest. The resulting uncertainty in χ_{eff} for the star–star blends is estimated as approximately $\pm 0.4 \times 10^{-4}$.

All the values of χ_{eff} for the star–star blends are larger than those for the isotopic blend of linear materials. The slope of the data for the four-arm star/four-arm star sample is the same as that of the data for the linear–linear blend. This suggests that the enthalpic contribution to χ_{eff} because of labeling is independent of architecture, as seen in star–linear PS blends.[19] In fact, the slopes of all the data for χ_{eff} versus $1/T$ presented in this article are similar, strengthening the argument that this is the case. There are some small differences in slope that appear in a self-consistent manner in separate experiments.[20] This self-consistency suggests there may be small additional enthalpic effects that differ slightly from architecture to architecture. These perturbations could conceivably be caused by the small differences in core structures of the different stars or by the different numbers of chain ends in the stars, and are the subject of additional study. The cores and chain ends are the only parts of the stars that are chemically distinct among the stars. As the number of arms increases from four to six, χ_{eff} decreases. The slope for the h6d6s data is distinct from that for the data from the blend of four-arm stars, suggesting a small enthalpic effect. For the blend of eight-arm stars, the values of χ_{eff} are comparable to those for the four-arm star blend, although the slope is more similar to that of the data from the six-arm star blend than that from the four-arm star blend. For the series of measurements represented in Figure 2, the microstructures are very consistent; therefore, there is no question that the behavior observed for this series of samples is somehow caused by differences in microstructure.

The variation in the value of χ_{eff} for a star–star blend with the number of arms in the star at a single temperature of 40 °C is summarized in the plot of Figure 3. Comparisons to corresponding linear–linear blends are made by treating them as blends of two-arm stars. The values of χ_{eff} for respective star–linear PB blends are also shown for comparison. Comparisons of the results from the star–star blends with previously reported[20] results from star–linear PB blend analogues over the entire temperature range previously reported[20] are made in Figure 4. For all three types of stars

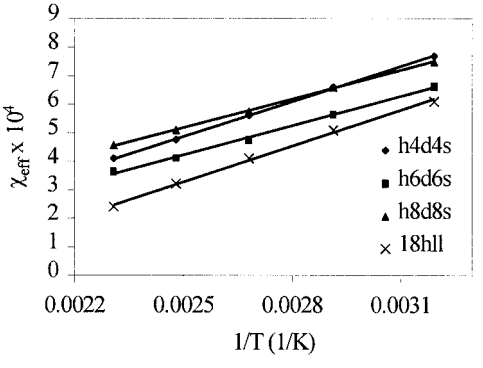

Figure 2. Interaction parameter as a function of inverse temperature for 19 vol % star hPB in a matrix of 81 vol % star dPB with the same number of arms. The sample, 18hll, 20 vol % linear hPB/80 vol % linear dPB is shown for comparison.

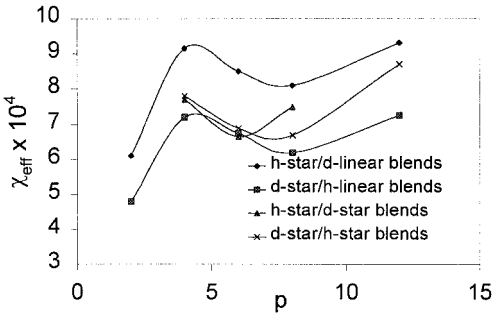

Figure 3. Plot of χ_{eff} as a function of the number of arms, p, in the stars for star–star blends in which the two stars have the same number of arms. The linear–linear blend is included for comparison by treating it as though it were a blend of two-arm stars.

(four-, six-, and eight-arm), the value of χ_{eff} for the star blend lies more or less between values for corresponding star–linear blends, one in which the star is deuterated and one in which the linear component is deuterated, moving up as the number of arms is increased from four to six to eight.

Overall, the values of χ_{eff} for the star–star blends compared more closely to values of χ_{eff} for the corresponding star–linear blends than to those for the comparable linear–linear blend. Although the architectures of the two star polymers are the same, an entropic contribution to the value of χ_{eff} is caused by the existence of the branch point and additional chain ends (both are part of the "architecture" effects). If the structure factor used is a good approximation for the stars, then the difference between the value of χ_{eff} for the star–star isotopic blend and the value of χ_{eff} for the linear–linear blend should give an estimate of the nonlocal effects induced by the presence of the junction and additional chain ends. A second possibility is that the true structure factor for the stars differs enough from the assumed form that the deviations manifest themselves in an apparent architectural contribution to the value of χ_{eff} for the star–star isotopic blend. We anticipate that the contribution to χ_{eff} from that sort of discrepancy would be more important for a larger number of arms, especially for the 12-arm star. It is not possible with this data set to eliminate that possibility as an alternative explanation of the data.

The junction point of the stars also played a role in the values of χ_{eff} for a series of star–star blends in which the number of arms was varied, just as previously discussed, but in which the minority component was deuterated. Scattering was measured for the following d-star/h-star blends: (1) 4-arm star dPB/4-arm star hPB (d4h4s), (2) 6-arm star dPB/6-arm star hPB (d6h6s), (3) 8-arm star dPB/8-arm star hPB

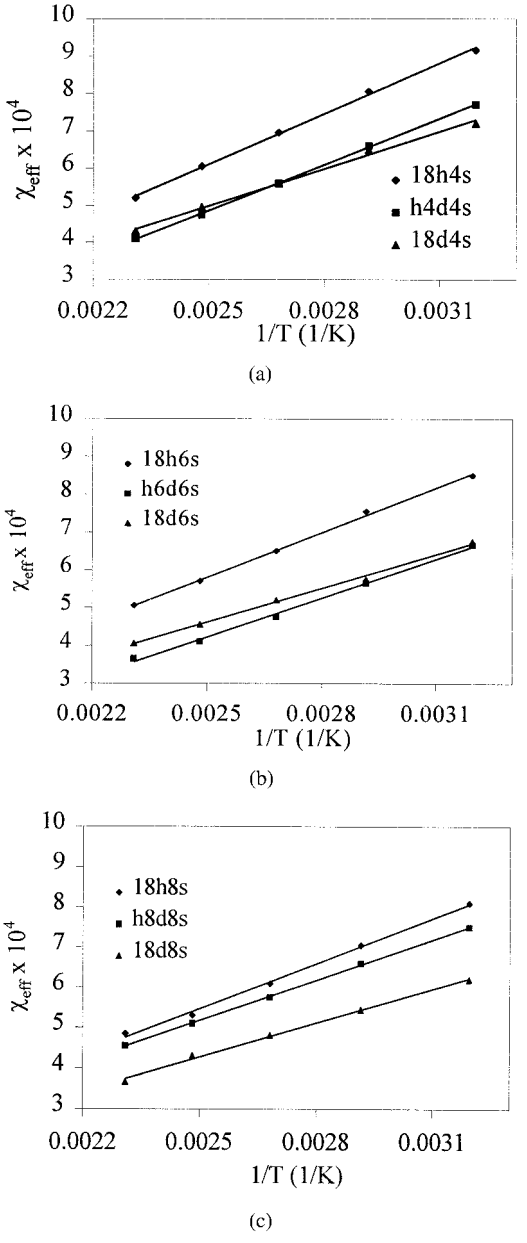

Figure 4. Interaction parameter as a function of inverse temperature for 19 vol % star hPB/81 vol % star dPB (same number of arms) as compared with their respective star–linear PB blends: (a) four-arm star–star PB blend as compared with four-arm star–linear PB blend, (b) six-arm star–star PB blend as compared with six-arm star–linear PB blend, and (c) eight-arm star–star PB blend as compared with eight-arm star–linear blend.

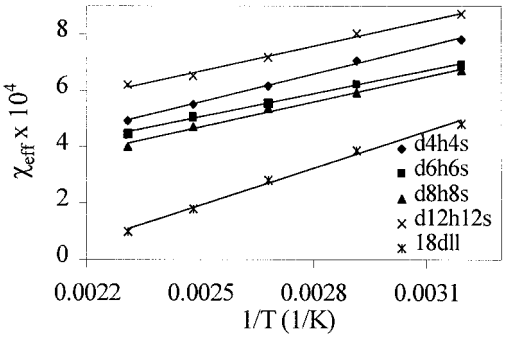

Figure 5. Interaction parameter as a function of temperature for 17 vol % star dPB in a matrix of 83 vol % star hPB with the same number of arms. The sample, 18dll, 20 vol % linear dPB/80% linear hPB is shown for comparison.

(d8h8s), and (4) 12-arm star dPB/12-arm star hPB (d12h12s). The values of χ_{eff} for these blends are shown in Figure 5 along with those for a 20/80 linear dPB (98 k)/linear hPB (87 k) blend (18 dll). Here the differences between the value of χ_{eff} for the star–star blends and the linear–linear blends are even larger. The presence of the junction points clearly increases the value of χ_{eff}. However, the ordering of the curves with number of arms in the stars is different than that seen in Figure 2. Here χ_{eff} decreases monotonically as the number of arms of the stars is changed from 4 to 6 to 8 and then increases when the number of arms of the stars is increased to 12. In fact, the value of χ_{eff} for the 12-arm star blend is higher than that for the 4-arm star blend. This trend in χ_{eff} with a change in number of arms is the same as that for the star–linear PB blends,[20] that is, in the star–linear PB blends with a deuterated star minority component χ_{eff} decreases as the number of arms decrease from 4 to 6 to 8, but then increases markedly for the case of 12 arms. It is possible that for the blends with the deuterated 4- and 12-arm stars there is a small contribution to χ_{eff} because of the microstructure mismatch between linear and star component. These two blends have the only significant mismatch. It is small and the same in the two cases. Differences in microstructures themselves can result in measurable values of χ_{eff} for isotopic blends of PB.[7–9,30] Thus, in the absence of branching or chain-end effects, the blends with the deuterated 4- and 12-arm stars would be expected to have values of χ_{eff} above those of the other star–star blends. In fact, if "raw" microstructure effects (unmitigated by architectural effects) were dominant, one would expect the values of χ_{eff} to be identical for the 4- and 12-arm blends, but this is not observed. The key trends in the data cannot be understood by appealing simply to arguments about microstructure mismatch.

Once again the slope of the data from the four-arm star blend appears to be somewhat different from that for the other blends. It seems unlikely that this is because of differences in core chemistries among the stars because each star has a different core, but the slopes of the data for the 6-, 8-, and 12-arm star blends are all very similar. It is also not because of chain-end chemistry because any enthalpic contribution from chain ends should become more prominent with an increasing number of arms. In fact, ongoing research[31] by the authors suggests that, among four possible chain-end chemistries studied so far, the butyl chain ends result in the smallest chain-end effects.

Overall, the values of χ_{eff} for the d-star/h-star blends are slightly larger than those found for the h-star/d-star blends except for sample d8h8s (Fig. 3). All the values of χ_{eff} for the star–star blends are in between those found for the corresponding d-star/linear PB blends and h-star/linear PB blends except for d12h12s. The value of χ_{eff} for d12h12s is 1.9×10^{-4} above the value of χ_{eff} for a corresponding 12-arm star dPB/linear hPB blend and 0.5×10^{-4} higher than χ_{eff} for a 12-arm star hPB/linear dPB blend at the highest temperature of 160 °C. Nonetheless, the values of χ_{eff} observed for the star–star blends more closely resemble those from the analogous star–linear PB blends than those from the isotopic linear–linear PB blend. From this series of measurements, it appears there is not only an isotopic effect but also an architecture (junction + chain ends) effect reflected in the magnitude of χ_{eff} for the star–star blends. The presence of the junction points and chain ends of the stars impacts the value of χ_{eff} even when the architectures of the two components have the same degree of branching.

Star–Star Blends of Components Having Different Numbers of Arms

To investigate how varying the number of arms in the star affect χ_{eff} in star–star blends, PB blends containing two star components with different numbers of arms were examined. Scattering was measured for the following blends: (1) six-arm star hPB/eight-arm star dPB (h6d8s), (2) four-arm star hPB/eight-arm star dPB (h4d8s), and (3)

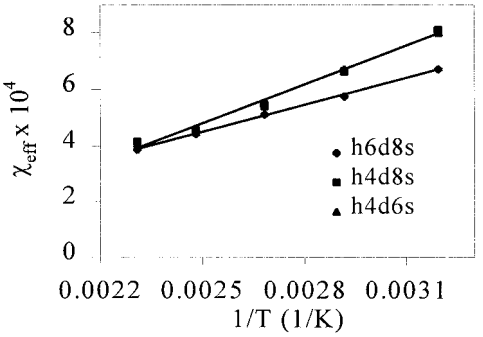

Figure 6. Interaction parameter as a function of temperature for 20 vol % star hPB in a matrix of 80 vol % star dPB with a different number of arms.

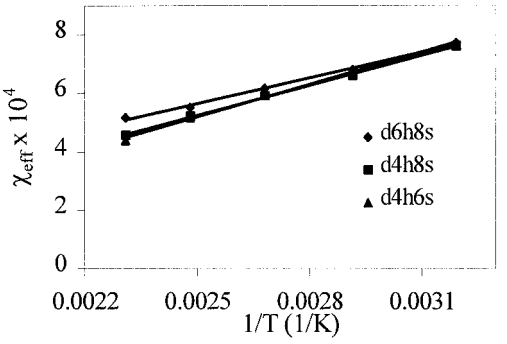

Figure 7. Interaction parameter as a function of temperature for 16 vol % star dPB in a matrix of 84 vol % star hPB with a different number of arms.

four-arm star hPB/six-arm star dPB (h4d6s). The corresponding temperature dependencies of χ_{eff} are shown in Figure 6. The values of χ_{eff} for the two samples in which the minority component is the four-arm star, h4d8s and h4d6s, are remarkably similar at all temperatures. This suggests that the four-arm star interacts identically with six- and eight-arm stars. However, experimentally significant differences between the values of χ_{eff} for h6d8s and the other two star–star blends are actually found only at the lowest temperatures. The slopes of the data sets for the blends containing four-arm stars are higher than the slope of the data for the sample without four-arm stars. When the matrix is an eight-arm star, χ_{eff} decreases upon increasing the branching of the minority component.

Similar trends were discovered for blends in which the minority component was deuterated (Fig. 7). Scattering was measured for three of the following star–star blends: (1) six-arm star dPB/eight-arm star hPB (d6h8s), (2) four-arm star dPB/eight-arm star hPB (d4h8s), and (3) four-arm star dPB/six-arm star hPB (d4h6s). Once again, similar values of χ_{eff} were found for all temperatures measured for the two samples containing four-arm stars, and the slopes are higher for the two blends containing the four-arm star. Overall, the results suggest that any differences in the interaction of the four-arm star with the six- and eight-arm stars are very small for arms of these lengths. The slope of the curve for sample d6h8s is very similar to that for sample h6d8s, as shown in Figure 8, but the curve for the d6h8s sample is about 1×10^{-4} higher, suggesting an entropic change in χ_{eff} with the "isotopic swap." Such an entropic contribution to χ_{eff} from swapping the labeling was also seen for star–linear PB blends,[20] but we are unable to explain the origin of this change.

With data in hand on both blends containing matching stars and blends containing asymmetric stars, a challenge to our understanding of the behavior of χ_{eff} emerges. If there are what we have termed "architectural effects" in the star–star blends, then χ_{eff} should change when the number of arms of one of the stars is altered. Changing the number of arms indeed alters the chain architecture. However, the fact that χ_{eff} does not change (or changes very little) when the number of arms changes suggests either that architectural effects are not playing a role or that the effect because of a change in the number of arms (for these comparatively long arms) is sufficiently smaller than the effect from the introduction of junction points that the experiments are simply unable to properly resolve it. We exclude

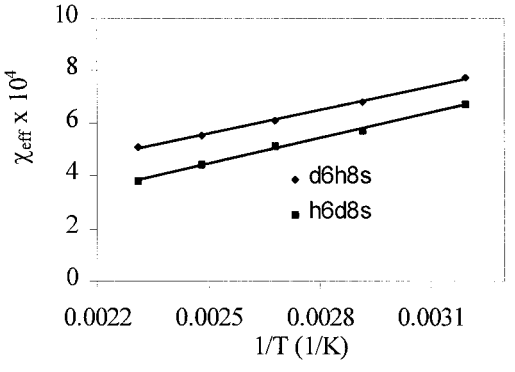

Figure 8. Interaction parameter as a function of temperature for a blend of 20 vol % six-arm star hPB/80 vol % eight-arm star dPB and for the "isotopic swap" blend of 16 vol % six-arm star dPB/84 vol % eight-arm star hPB.

the possibility that these differences in values of χ_{eff} are due to the approximations in the structure factors being used to deduce the values of χ_{eff}. Contributions to the value of χ_{eff} because of approximations in the structure factor should change when the number of arms in one star is changed because the degree of approximation grows more and more severe as the number of arms in the star is increased. The fact that χ_{eff} does not change appreciably with the number of arms in the second star indicates that approximation of the structure factor is not the primary issue. Rather, we expect that architectural effects because of numbers of arms are simply too subtle here to sort out.

CONCLUSIONS

The values of χ_{eff} derived from SANS of isotopic blends with an RPA approach and structure factors ignoring arm stretching are higher for star–star blends than for corresponding linear–linear blends. This suggests that the addition of the junction point in the chain architecture affects the value of χ_{eff} even in isotopic blends in which the two components have the same architecture. Changing the number of arms on one of the components in a star–star blend had little impact on the value of χ_{eff}. Most likely the changes because of increasing the number of arms by no more than a factor of two are too subtle to be resolved by the approach used here.

The authors gratefully acknowledge financial support from the Army Research Office (contract DAAH04-96-1-0164). T. D. Martter thanks the LORD Corp. for a graduate fellowship. The authors acknowledge the support of the NIST, U.S. Department of Commerce, in providing the neutron facilities supported through NSF-DMR-9423101. The authors also thank P. Butler for his help with the SANS experiments. Samples of *sec*-BuLi were provided by FMC, Lithium Division.

REFERENCES AND NOTES

1. Fredrickson, G. H.; Liu, A.; Bates, F. S. Macromolecules 1994, 27, 2503–2511.
2. deGennes, P. G. Scaling Concepts in Polymer Physics; Cornell University Press: Ithaca, NY, 1979.
3. Bates, F. S.; Wignall, G. D.; Koehler, W. C. Phys Rev Lett 1985, 55, 2425–2428.
4. Bates, F. S.; Dierker, S. B.; Wignall, G. D. Macromolecules 1986, 19, 1938–1945.
5. Bates, F. S.; Wignall, G. D. Phys Rev Lett 1986, 57, 1429–1432.
6. Hopkinson, I.; Kiff, F. T.; Richards, R. W.; King, S. M.; Munro, H. Polymer 1994, 35, 1722–1729.
7. Sakurai, S.; Jinnai, H.; Hasegawa, H.; Hashimoto, T.; Glen Hargis, I.; Aggarwal, S. L.; Han, C. C. Macromolecules 1990, 23, 451–459.
8. Jinnai, H.; Hasegawa, H.; Hashimoto, T.; Han, C. C. Macromolecules 1992, 25, 6078–6080.
9. Sakurai, S.; Jinnai, H.; Hasegawa, H.; Hashimoto, T.; Han, C. C. Macromolecules 1991, 24, 4839–4843.
10. Lee, M. H.; Fleischer, C. A.; Morales, A. R.; Koberstein, J. T.; Koningsveld, R. Polymer 2001, 42, 9163–9172.
11. Alamo, R. G.; Graessley, W. W.; Krishnamoorti, R.; Lohse, D. J.; Londono, J. D.; Mandelkern, L.; Stehling, F. C.; Wignall, G. D. Macromolecules 1997, 30, 561–566.
12. Chen, Y. Y.; Lodge, T. P.; Bates, F. S. J Polym Sci Part B: Polym Phys 2000, 38, 2965–2975.
13. Faust, A. B.; Sremcich, P. S.; Gilmer, J. W.; Mays, J. W. Macromolecules 1989, 22, 1250–1254.
14. Russell, T. P.; Fetters, L. J.; Clark, J. C.; Bauer, B. J.; Han, C. C. Macromolecules 1990, 23, 654–659.
15. van Aert, H. A. M.; Genderen, M. H. P.; Meijer, E. W. Polym Bull 1996, 37, 273–280.
16. Tsukahara, Y.; Inoue, J.; Ohta, Y.; Kohjiya, S. Polymer 1994, 35, 5785–5789.
17. Greenberg, C. C.; Foster, M. D.; Turner, C. M.; Corona-Galvan, S.; Cloutet, E.; Butler, P. D.; Hammouda, B.; Quirk, R. P. Polymer 1999, 40, 4713–4716.
18. Foster, M. D.; Greenberg, C. C.; Teale, D. M.; Turner, C. M.; Corona-Galvan, S.; Cloutet, E.; Butler, P. D.; Hammouda, B.; Quirk, R. P. Macromol Symp 2000, 149, 263–268.
19. Greenberg, C. C.; Foster, M. D.; Turner, C. M.; Corona-Galvan, S.; Cloutet, E.; Quirk, R. P.; Butler, P. D.; Hawker, C. J Polym Sci Part B: Polym Phys 2001, 39, 2549–2561.
20. Martter, T. D.; Foster, M. D.; Yoo, T.; Xu, S.; Lizzaraga, G.; Quirk, R. P.; Butler, P. D. Macromolecules, accepted for publication.
21. In reference 18 there are typographical errors in the last column of Table 3. The entries in rows 6–11 for the theoretically predicted contribution are all missing a trailing "0," that is, the printed quantities are too small by a factor of 10.
22. Horton, J. C.; Squires, G. L.; Boothroyd, A. T.; Fetters, L. J.; Rennie, A. R.; Glinka, C. J.; Robinson, R. A. Macromolecules 1989, 22, 681–686.
23. Hutchings, L. R.; Richards, R. W. Macromolecules 1999, 32, 880–891.

24. Benoît, H. C. J Polym Sci 1953, 11, 507.
25. Hseih, H. L.; Quirk, R. P. Anionic Polymerization; Marcel Dekker: New York, 1996, p 333.
26. Grest, G. S.; Fetters, L. J.; Huang, J. S.; Richter, D. Advances in Chemical Physics. In Polymeric Systems; Prigogine, I.; Rice, S. A., Eds.; Wiley: New York, 1996; Vol. 94, pp 67–163.
27. Douglas, J. F.; Roovers, J.; Freed, K. F. Macromolecules 1990, 23, 4168–4180.
28. Bates, F. S.; Schulz, M. F.; Rosedale, H. H.; Almdal, K. Macromolecules 1992, 25, 5547–5550.
29. Polymer Handbook, 4th ed.; Brandup, J.; Immergut, E. H.; Grulke, E. A., Eds.; Wiley: New York, 1999, p V-1.
30. Schwahn, D.; Willner, L. Macromolecules 2002, 35, 239–247.
31. Hwang, J. H.; Foster, M. D. Bull Am Phys Soc 2002, 47, 841.